Int. J. Electrochem. Sci., 6 **(2011)** 1438 - 1453

International Journal of
ELECTROCHEMICAL
SCIENCE
www.electrochemsci.org

Impedimetric Response of a Label-Free Genosensor Prepared on a 3-Mercaptopropionic Acid Capped Gallium Selenide Nanocrystal Modified Gold Electrode

Peter M. Ndangili[*], *Abongile N. Jijana, Rasaq A. Olowu, Stephen N. Mailu, Fanelwa R. Ngece, Avril Williams, Tesfaye T. Waryo, Priscilla G.L. Baker, Emmanuel I. Iwuoha*.*

SensorLab, Department of Chemistry, University of the Western Cape, Private Bag X17, Bellville, 7535, South Africa.
[*]E-mail: pndangili@uwc.ac.za; eiwuoha@uwc.ac.za

Received: 9 March 2011 / *Accepted:* 11 April 2011 / *Published:* 1 May 2011

Biocompatible and water soluble 3-mercaptopropionic acid capped gallium selenide nanocrystals were synthesized from hydrated gallium (III) perchlorate and selenide ions. The nanocrystals were non-fluorescent but showed a sharp UV-vis absorption maximum at 260 nm. Transmission electron micrographs showed the formation of high quality non-aggregated particles with an average diameter of 65 nm. Gold electrode modified with the capped nanocrystals was used as a platform for impedimetric genosensing using NH_2-5′-CCCACCGGTCCTTCATGTTC-3′ (probe) and 5′-GAACATGAAGGA CCGGTGGG-3′ (target) oligonucleotide sequences. The target oliginucleotide sequence is a component of 5-enolpyruvylshikimate-3-phosphate synthase, a common vector gene in glyphosate resistant transgenic plants. The impedimetric genosensor exhibited high sensitivity towards the target DNA (sensitivity = 11.61 Ω/nM) with a detection limit of 0.66 nM (3s, n = 8). The genosensor was able to discriminate between complementary, non-complementary and 3-base mismatched target sequences and maintained 87 % of its response towards the target DNA after one month.

Keywords: Gallium selenide, impedimetric genosensor, transmission electron microscopy (TEM), electrochemical impedance spectroscopy (EIS), 5-enolpyruvylshikimate-3-phosphate synthase (CP4 espsp).

1. INTRODUCTION

Metal selenide semiconducting nanoparticles produced from groups III and VI elements have attracted a lot of research attention due to their potential use as alternatives to nanomaterials from

groups II and VI used in electrical, nonlinear optical, optoelectronic and photovoltaic devices [1-2]. Synthesis of gallium selenide has been achieved through molecular beam epitaxy [3], vapour phase epitaxy [4], chemical vapour deposition (CVD) [5], heterovalent exchange reaction involving groups V and V elements [6], thermal evaporation [7] and chemical close-spaced vapour transport [8], among others. These methods give rise to water insoluble and bio-incompatible materials that cannot find applications in bioanalytical chemistry. Synthesis of water soluble and bio-compatible gallium selenide nanocrystals would therefore open the applications of these materials in several areas including biotechnology, health care, biomedical and pharmaceutical industries as well as in bioanalytical chemistry. Water soluble gallium selenide nanocrystals have not been explored due to the rare cationic chemistry of aqueous Ga^{3+}. Whereas compounds of gallium in its univalent oxidation state have been reported [9], details of cationic existence of Ga^{3+} are scanty. In this work, the reaction between hot perchloric acid and gallium, according to equation 1, is presented as a source of Ga^{3+} for synthesis of gallium selenide nanocrystals (NCS).

$$2Ga + 6HClO_4 + 6H_2O \rightarrow 2Ga(ClO_4)_3.6H_2O + 3H_2 \qquad (1)$$

Short amphiphilic bifunctional molecules such as mercaptopropionoc acid (MPA) are suitable capping materials for nanocrystals since they allow bioconjugation, solubilization, rapid transfer of electrons and enhanced electrochemical responses of the nanocrystals to target analytes [10]. Although nanocrystals show excellent electrochemical properties when functionalized, their use in electrochemical systems for analytic purposes has been very limited [11-13].

The detection of transgenic DNA in food products made from genetically modified organisms (GMOs) has recently become one of the mostly requested DNA-sensor applications. [14, 15]. This is due to: (i) the potential alterations in nutritional composition of GMO food and the functions of non-targeted genes; (ii) allergenicity or toxicity of the genetically modified product; and (iii) the possibility of horizontal gene transfer to non-targeted species and to the environment [16]. Recombinant DNA from GMOs has been found in air [17, 18], soil [19-21] as well as in the food chain [22-27]. The gene 5-enolpyruvylshikimate-3-phosphate synthase (CP4 epsps) is commonly used in genetic engineering of crops as a vector gene to confer glyphosate resistance in transgenic plants. In many parts of the world, legislations have been put in place to regulate the presence of genetically modified organisms in crops, foods and ingredients [28]. This has necessitated development of sensitive and reliable methods for detection, identification and quantification of genetically modified organisms (GMOs) in processed food. Various methods including quartz crystal microbalance [29, 30], surface plasmon resonance [31, 32], fluorescence [33] and electrochemistry [34] have been reported for DNA detection. Among these methods, electrochemical detection of DNA has received extensive attention due to its high sensitivity, excellent selectivity, simple instrumentation, rapidity and low production cost [35-38]. Most electrochemical DNA biosensors are based on electrical transduction of DNA hybridization by an accompanied accumulation of redox compounds such as dyes (methylene blue [39, 40]) or metal complexes (ruthenium and osmium complexes [41]) at the DNA-modified electrode surface [42]. The hybridization reaction can be monitored by intrinsic signals of nucleic acids or electroactive labels such as enzymes and metal nanoparticles covalently bound to the target DNA [43, 44] or by changes in

interfacial properties [35, 45] such as conductance, resistance [46-48] and capacitance [47]. Electrical resistance and capacitance are sensitive indicators of surface properties and are suitable for the interrogation of DNA hybridization by electrochemical impedance spectroscopy (EIS) technique. This work reports a label-free impedimetric genosensor prepared on gold electrode that is modified with 3-mercaptopropionic acid-capped gallium selenide nanocrystals. The gallium selenide nanocrystals were used to create a large surface area on the electrode surface which ensured high loading of the probe DNA and improved rate of DNA hybridization on the electrode.

2. EXPERIMENTAL

2.1. Materials and apparatus

Analytical grade zinc nitrate hexahydrate, 3-mercaptopropionic acid ($HSCH_2CH_2CO_2H$) [3-MPA], sodium hydroxide, selenium powder, sodium borohydrate, disodium hydrogen phosphate, sodium dihydrogen phosphate, potassium ferricyanide, potassium ferrocyanide, 1-ethyl-3-(3-dimethylaminopropyl) carbodiimide hydrochloride (EDC), N-hydroxysuccinimide (NHS), tris-EDTA buffer (10 mM Tris-HCl and 1 mM EDTA, pH 8.00), gallium and perchloric acid were all purchased from Sigma-Aldrich (Cape Town, South Africa). 0.10 M phosphate buffer solution, pH 7.40, was prepared from disodium hydrogen phosphate and sodium dihydrogen phosphate. 5.00 mM $[Fe(CN)_6]^{3-/4-}$ was prepared from $K_4Fe(CN)_6$ and $K_3Fe(CN)_6$ in a 1:1 ratio. 20 bases oligonucleotide sequences were purchased from Inqaba Biotechnical Industries (Pty) Ltd., Hatfield, South Africa. An amine terminated DNA with the sequence NH_2-5′-CCCACCGGTCCTTCATGTTC-3′ was used as the probe DNA while the sequence 5′-GAACATGAAGGACCGGTGGG-3′, which is a section of 5-enolpyruvylshikimate-3-phosphate synthase (CP4 espsp) gene of GMOs, was used as the complementary sequence. The non complementary and 3-base mismatch oligonucleotides were 5′-CATAGTTGCAGCTGCCACTG-3′ and 5′-GATCATGAAGCACCGGAGGG-3′, respectively. The oligonucleotide stock solutions were prepared with tris-EDTA buffer and stored in a freezer at 20 °C when not in use.

All voltammetric experiments were performed on a BAS100W electrochemical workstation from BioAnalytical Systems Incorporated (Lafayette, USA) using a three electrode system. Bare or modified gold electrode (Au|Ga_2Se_3-3MPA, or Au|Ga_2Se_3-3MPA|ssDNA) was used as the working electrode. Platinum wire and Ag|AgCl (3 M NaCl) were used as counter and reference electrodes, respectively. Electrochemical impedance spectroscopy (EIS) measurements were recorded with VoltaLab PGZ 402 from Radiometer Analytical (Lyon, France).

Transmission electron microscopy (TEM) studies were performed on samples of gallium selenide nanocrystals mounted on a copper coated TEM grid using a Tecnai G^2 F20X-Twin MAT 200 kV Field Emission Transmission Electron Microscope from FEI Eindhoven, Netherlands. Ultra violet-visible (UV-vis) absorption measurements were made on a Nicolet Evolution 100 UV–visible spectrometer (Thermo Electron, UK), using a quartz cuvette.

2.2. Synthesis of 3-mercaptopropionic acid capped Ga_2Se_3 nanocrystals.

4.87 g of Ga metal was weighed into a round bottomed flask and 2 mL of concentrated $HClO_4$ added. The mixture was refluxed under constant stirring for 4 h at 120 °C, after which, a white precipitate of $Ga(ClO_4)_3.6H_2O$ was formed. 0.19 g of the gallium salt was dissolved in 10 mL of distilled water and 69.60 µL of concentrated MPA added. The pH of the solution was adjusted to 12 using NaOH and saturated with N_2 for 30 min. Se^{2-} was prepared by mixing 0.016 g of Se powder with 0.015 g of $NaBH_4$ in a round bottomed flask and adding de-ionized water to make 10 mL solution, resulting to 0.02 M and 0.04 M of Se and $NaBH_4$, respectively. The mixture was then stirred continuously at room temperature under nitrogen saturation for 25 min after which a dark yellow solution was formed. Freshly prepared Se^{2-} was added drop wise into the nitrogen saturated $Ga(ClO_4)_3$/3MPA solution. After 10 min, a brown solution was formed and the reaction was quenched by immediately placing the reaction flask in a freezer at -20 °C.

2.3. Preparation of electrode.

A gold disk electrode was thoroughly cleaned by polishing it on a soft polishing pad using 1.00, 0.30 and 0.05 µM slurries of alumina, respectively, while rinsing with de-ionized water after each polish. This was followed by ultrasonication in de-ionized water for 5 min. The freshly polished gold was electrochemically cleaned in 0.50 M H_2SO_4 by potential scanning between −300 and +1500 mV until reproducible cyclic voltammograms were obtained.

The gold electrode was immersed in a Ga_2Se_3-3MPA solution for 12 h in the dark to form Au|Ga_2Se_3-3MPA. The modified electrode was then removed from the Ga_2Se_3-3MPA solution and gently rinsed with de-ionized water to remove any physically or weakly adsorbed nanocrystals. The Au|Ga_2Se_3-3MPA electrode was then immersed in a mixture of phosphate buffer (pH 7.40) solution of 5.00 mM EDC and 8.00 mM NHS for 30 min to obtain an active surface. The surface-activated electrode was rinsed gently with de-ionized water. 10 µL of 20 µM probe ssDNA solution was dropped on the modified solution and left to immobilize for 12 h at 25 °C to give Au|Ga_2Se_3-3MPA|ssDNA genosensor system.

2.4. Hybridization and electrochemical detection

The DNA potentiostatic hybridization reaction was performed by dipping the biosensor in a stirred solution (0.10 M phosphate buffer, pH 7.40) containing different concentrations of the target (complementary) DNA at a potential of 500 mV for 10 min. The hybridized electrode was washed twice with phosphate buffer solution. The same procedure was repeated using the non-complementary or the 3-base mismatch oligonucleotides instead of the complementary DNA. Electrochemical detection was done by performing EIS of the genosensor in the presence and absence of target DNAs (complementary, non-complementary and 3-base mismatch) using 5.00 mM $[Fe(CN)_6]^{3-/4-}$ as the redox indicator. The impedimetric spectra were recorded with a VoltaLab PGZ 402 at a frequency range of 50 kHz to 100 mHz, amplitude of 10 mV and a potential of 200 mV.

3. RESULTS AND DISCUSSION

3.1. Spectroscopy of the Ga_2Se_3-3MPA nanocrystals

The UV-vis absorption spectrum of the Ga_2Se_3-3MPA (Fig. 1) shows a sharp absorption maxima at 260 nm, which is due to the presence of a zinc-blend-type defect in Ga_2Se_3 [1]. Usually, the nature of the interaction between the conduction and valence bands as well as the size of the band gap determine the optical properties of a semiconducting nanocrystal. The absorption of a photon by a Ga_2Se_3 nanocrystal causes electronic transition from the valence band to the conduction band, which creates an electron-hole pair known as an exciton in the valence band. The lowest-energy electron-hole pair (excitonic) state ($1S_{3/2}$-$1S_e$) is not usually observable in nanocrystals that are heterogeneous in size, shape and composition. However, more homogeneous nanocrystals exhibit characteristic sharp absorption peaks. The UV-vis maximum at 260 nm (Fig. 1), therefore, shows that Ga_2Se_3-3MPA nanocrystals are homogeneous in particle size distribution.

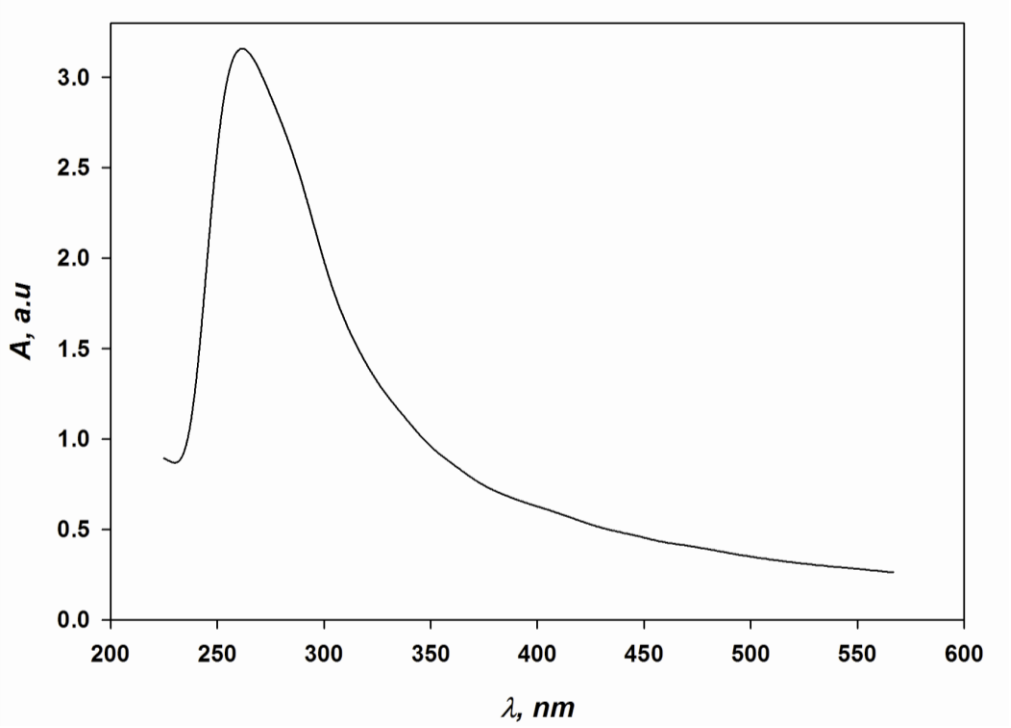

Figure 1. UV-vis spectrum of Ga_2Se_3-3MPA nanoparticles.

The transmission electron micrographs of the Ga_2Se_3-3MPA nanoparticles (Fig. 2) show the formation of high quality non-aggregated particles with an average diameter of 65 nm. Non-aggregation of the nanocrystals is believed to have resulted from the electrostatic repulsion of negatively charged dehydrogenated carboxyl groups present in the 3-MPA [49].

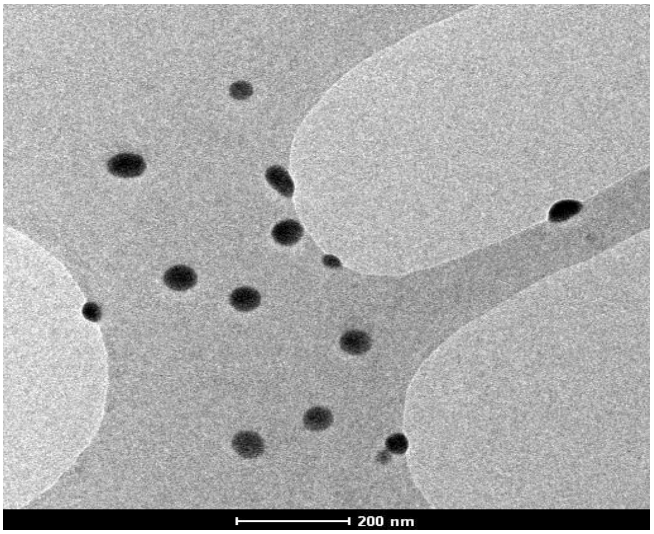

Figure 2. TEM micrograph of Ga_2Se_3-3MPA nanoparticles.

3.2. Electrochemical interrogation of the Ga_2Se_3-3MPA nanocrystals

3.2.1 Electrochemistry of adsorbed Ga_2Se_3-3MPA in 0.1 M phosphate buffer of pH 7.40 as well as in 5.00 mM $Fe(CN)_6^{3-/4-}$

Electrochemical impedance spectroscopy is a well known technique for interrogating interfacial electrical properties of surface modified electrodes. Figure 3 below depicts the Nyquist plots for bare Au and Au|Ga_2Se_3-3MPA in 5.00 mM $Fe(CN)_6^{3-/4-}$. The figure also shows the corresponding Randle's equivalent circuit consisting of a solution resistance (R_s), charge transfer resistance (R_{ct}), Warburg impedance (Z_w) and constant phase element (CPE_{dl}). R_{ct} represents the resistance to the charge transfer between the electrolyte and the electrode and contains information on the electron transfer kinetics of the redox probe at the electrode interface. The R_{ct} values of bare Au and Au|Ga_2Se_3-3MPA electrodes were 718 ± 1.74 Ω and 3338 ± 0.66 Ω, respectively. This represents a four-fold increase in R_{ct} value when Au electrode was modified with Ga_2Se_3-3MPA nanocrystals. The increase in R_{ct} value could be due to the electrostatic repulsion between the Ga_2Se_3-3MPA and $Fe(CN)_6^{3-/4-}$ redox probe which are both negatively charged. The surface coverage (θ) of Ga_2Se_3-3MPA on gold electrode was calculated from equation 2 [50-51] and found to be 0.78.

$$\theta = 1 - \frac{R_{ct}^{Bare}}{R_{ct}^{Au/ZnSe-3MPA}} \qquad (2)$$

where R_{ct}^{Bare} and $R_{ct}^{Au/ZnSe-3MPA}$ are the charge transfer resistance of the bare Au and Au|Ga_2Se_3-3MPA electrodes, respectively. A comparative analysis of the interfacial heterogeneous electron transfer rate of the bare Au and the Au|Ga_2Se_3-3MPA electrodes was done using equations 3a and 3b [52]:

$$R_{ct} = \frac{RT}{nFi_o} \quad (3a)$$

$$i_o = nFAk^0C^* \quad (3b)$$

where n is the number of electrons transferred, F is the Faraday constant (96,584 C mol^{-1}), R is the gas constant (8.314 J mol^{-1} K^{-1}), T is the reaction temperature (298 K), i_o is the standard exchange current (A), A is the geometric area of the electrode (0.02 cm^2), k^0 is the heterogeneous rate transfer constant (cm s^{-1}) and C^* is the concentration of $Fe(CN)_6^{3-/4-}$ (5.00 mM). The values of i_o for the bare Au and Au|Ga_2Se_3-3MPA electrodes were 3.58 x 10^{-5} A and 7.69 x 10^{-6} A, respectively and the corresponding k^0 values were 3.69 x 10^{-3} cm s^{-1} and 7.93 x 10^{-4} cm s^{-1}. The larger value of k^0 for Au electrode supports the theory that the semi-conducting Ga_2Se_3-3MPA impeded the charge transfer of the $Fe(CN)_6^{3-/4-}$ redox probe.

Cyclic voltammetry of the Au|Ga_2Se_3-3MPA electrode in $Fe(CN)_6^{3-/4-}$ (Fig. 4) showed a wider redox peak separation (ΔE_p) than for Au (from 137 mV for Au to 324 mV for Au|Ga_2Se_3-3MPA) and a 49 % decrease in peak currents. The cyclic voltammetric behaviour of the modified electrode indicates

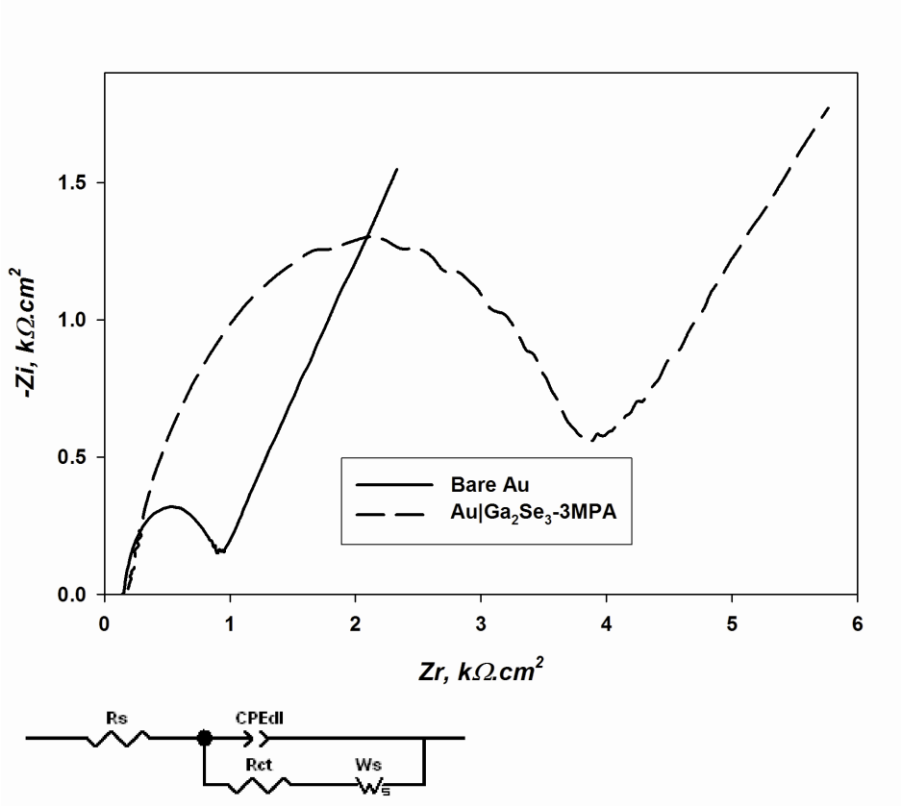

Figure 3. Nyquist plot of bare Au and Au|Ga_2Se_3-3MPA in 5.00 mM $Fe(CN)_6^{3-/4}$, with Randles equivalent circuit.

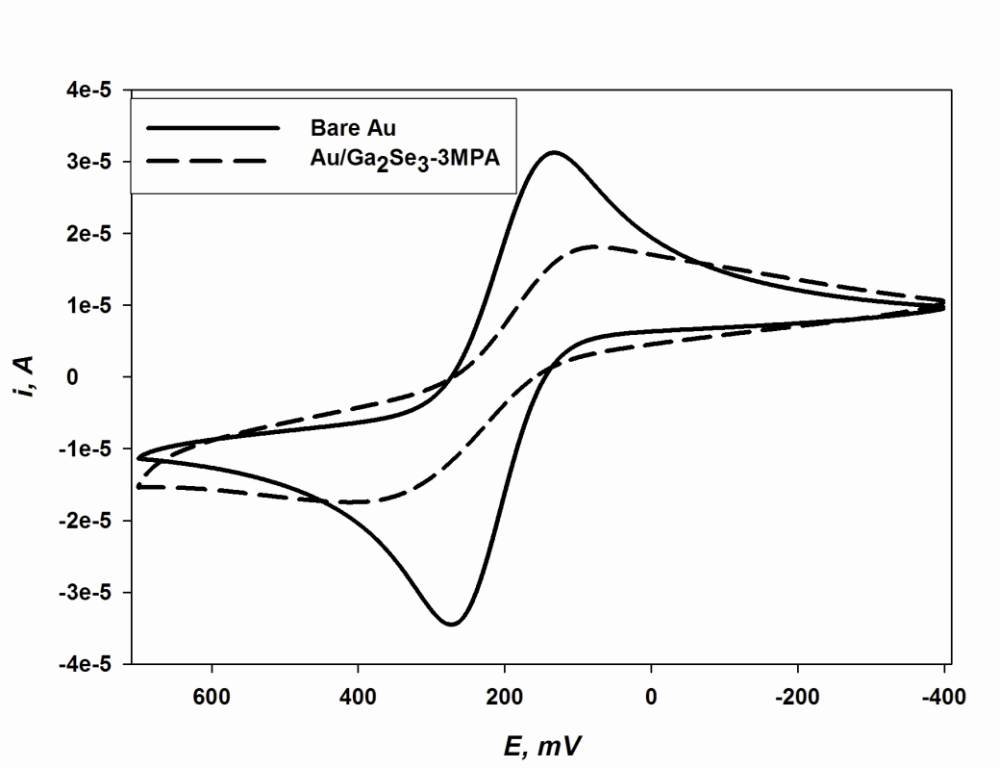

Figure 4. Cyclic voltammograms of bare Au and Au|Ga_2Se_3-3MPA in 5.00 mM $Fe(CN)_6^{3-/4}$ at 100 mV/s

a more sluggish electron transfer rate at the Ga_2Se_3-3MPA|$Fe(CN)_6^{3-/4}$ interface compared to Au|$Fe(CN)_6^{3-/4}$ and corroborates the electrostatic repulsion phenomenon observed in EIS. Figure 5 shows the cyclic voltammograms of the Au|Ga_2Se_3-3MPA in 0.10 M PBS of pH 7.40. It can be seen that the peak currents (i_p) increased linearly with increasing scan rate (ν) as shown in Fig.5 inset, which indicates the occurrence of the electrochemistry of surface confined species. The value of the slope of the linear plot of log ν versus log i_p can be used to elucidate the nature of the processes influencing the electrochemistry of the surface confined material. Slopes with values of 1.0 and 0.5 refer to adsorption-controlled and diffusion-controlled electrochemical processes, respectively. Intermediate values for the slope indicate mixed diffusion/adsorption-controlled processes [53]. In this work, the plots of log ν versus log i_p (not shown) gave slopes of 1.04 and 1.14 for the anodic and cathodic peaks, respectively which confirmed the occurrence of adsorption-controlled electrochemistry of the Ga_2Se_3-3MPA system.

In order to estimate the number of electrons transferred, equation 4a (Laviron's equation) [54] and equation 4b [55] were re-expressed to give equation 4c;

$$i_p = \frac{\omega n^2 F^2 A \Gamma \nu}{4RT} \qquad (4a)$$

$$Q = nFA\Gamma \qquad (4b)$$

$$i_p = \frac{nFQ\nu}{4RT} \qquad (4c)$$

where ω is the angular frequency, Γ is the surface concentration of the electrode material (Ga_2Se_3-3MPA, mol cm^{-2}), A is the electrode area (cm^2) and Q is the quantity of charge (C) calculated from the reduction peak area of the voltammogram; and n, i_p, F, R and T have their usual meanings. From the slopes of the i_p versus *ν* plots, n was calculated to be 0.98 and 1.14 for the anodic and cathodic processes, respectively, indicating that Ga_2Se_3-3MPA nanocrystals undergo a one-electron redox reaction at the Au electrode in phosphate buffer.

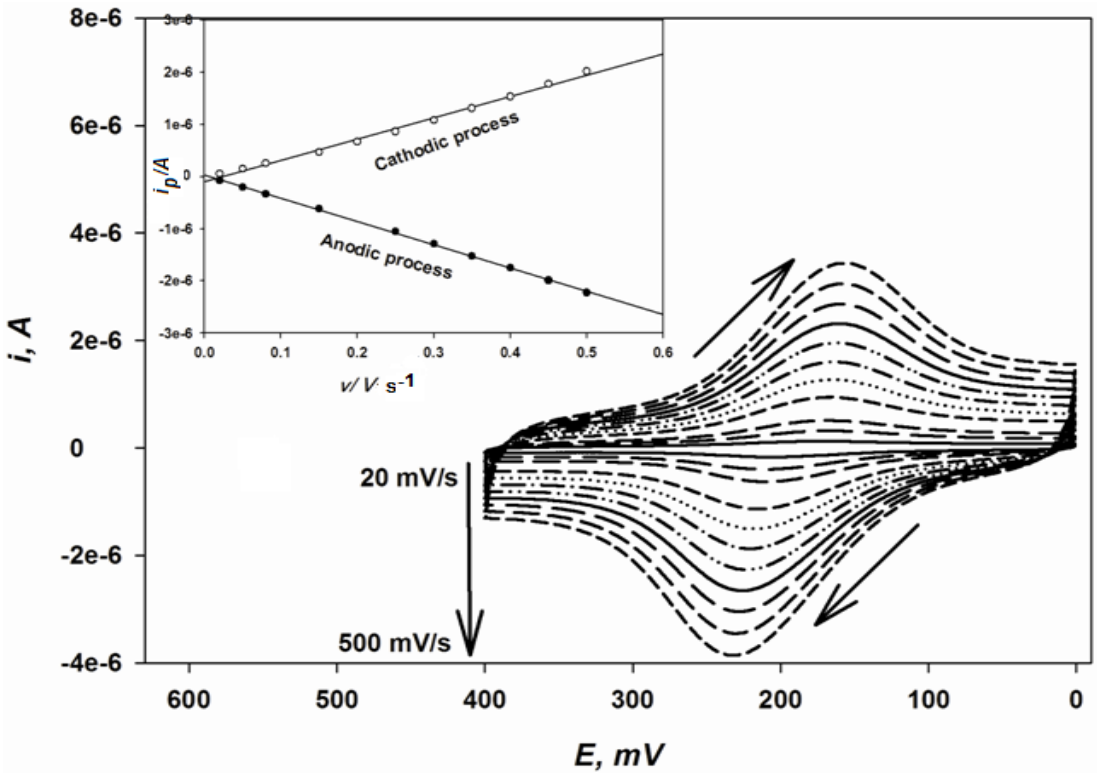

Figure 5. Cyclic voltammograms of Au|Ga_2Se_3-3MPA in 0.10 M phosphate buffer of pH 7.40: Inset; anodic and cathodic plots of peak current versus scan rate.

The average value for the ratio of cyclic voltammetric anodic to cathodic peak currents of Au|Ga_2Se_3-3MPA in buffer was 1.29, which indicates a one-electron quasi-reversible electrochemistry [56]. The surface concentration of Ga_2Se_3-3MPA, calculated from equation 4b, was 6.14 x 10^{-10} mol cm^{-2}. The ΔE_p values were found to be linear with the square root of scan rate (r^2 = 0.99), which is as expected for a quasi-reversible process [57]. The formal potential {$E^0 = (E_{p,a} + E_{p,c})/2$} was unaffected by the scan rate (SD = 1.21 x10^{-3} for 11 scan rates). This is an indication that the electron transfer coefficients, α_a and α_c for anodic and cathodic processes, respectively, are similar ($\alpha_a \approx \alpha_c \approx 0.5$).

3.2.2 Electrochemistry of Ga_2Se_3-3MPA in solution

The cyclic voltammetry of Ga_2Se_3-3MPA solution on gold electrode was studied at a potential range of -200 to +800 mV and the results are shown in Figure 6. An anodic peak (A_1) whose potential shifted inconsistently with scan rate is attributed to the oxidation of surface defects of Se to form intra-band surface states [58].

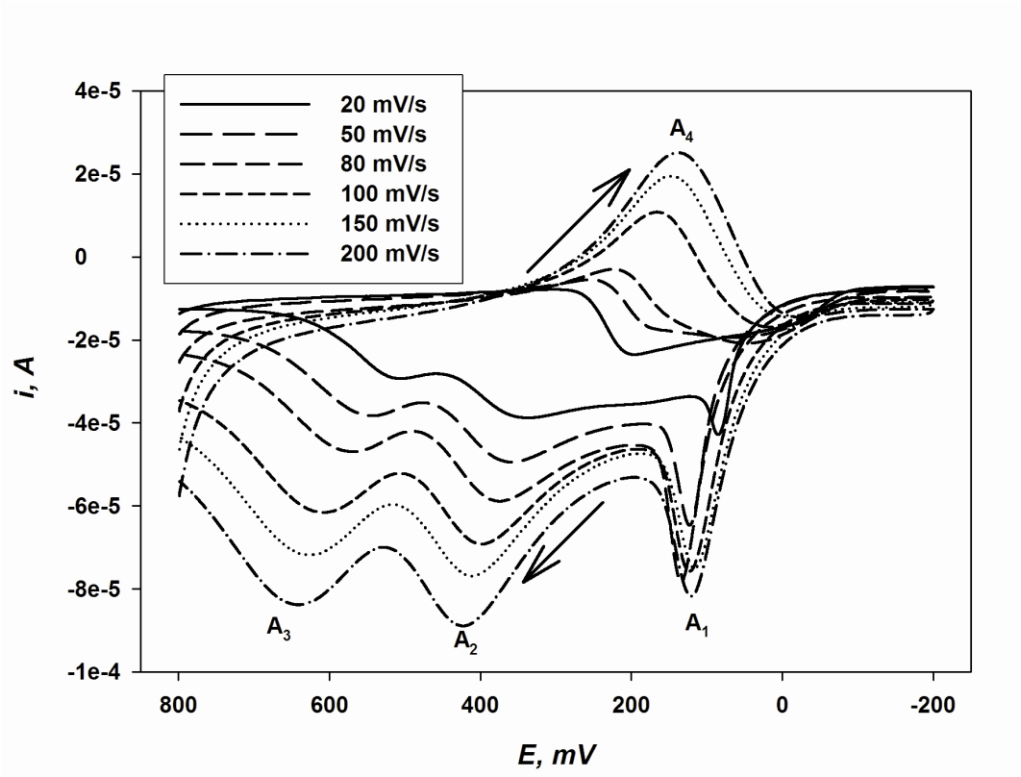

Figure 6. Cyclic voltammograms of Ga_2Se_3-3MPA solution.

The anodic peaks A_2 and A_3 shifted to more positive potentials with increasing scan rate, suggesting an irreversible behavior of the processes responsible for these peaks. Peak A_2 results from anodic stripping of elemental Se, arising from electro-oxidation of Se-related surface states [59]. A plot of log peak current versus log scan rate for this peak showed a linear relationship with a slope of 0.80 (r^2 = 0.99), indicating an adsorption-diffusion controlled reaction. A similar plot for peak A_3 was non linear but its current was found to be linearly dependent on the root of the scan rate from 50 mV/s to 500 mV/s. This indicates diffusion-controlled electrochemical reaction and may be attributed to the oxidation of the rest of the Ga_2Se_3 core. In the reverse scan, only one peak (A_4) was observed. The peak gave adsorption-controlled peak current-scan rate relationship, associated with the reduction of surface-bound Se species.

3.3. Impedimetric characteristics of the DNA modified electrode

Figure 7 below depicts the Bode (a) and Nyquist (b) plots for bare Au, Au|Ga_2Se_3-3MPA, Au|Ga_2Se_3-3MPA|ssDNA and Au|Ga_2Se_3-3MPA|dsDNA, all in 5.00 mM $Fe(CN)_6^{3-/4-}$.

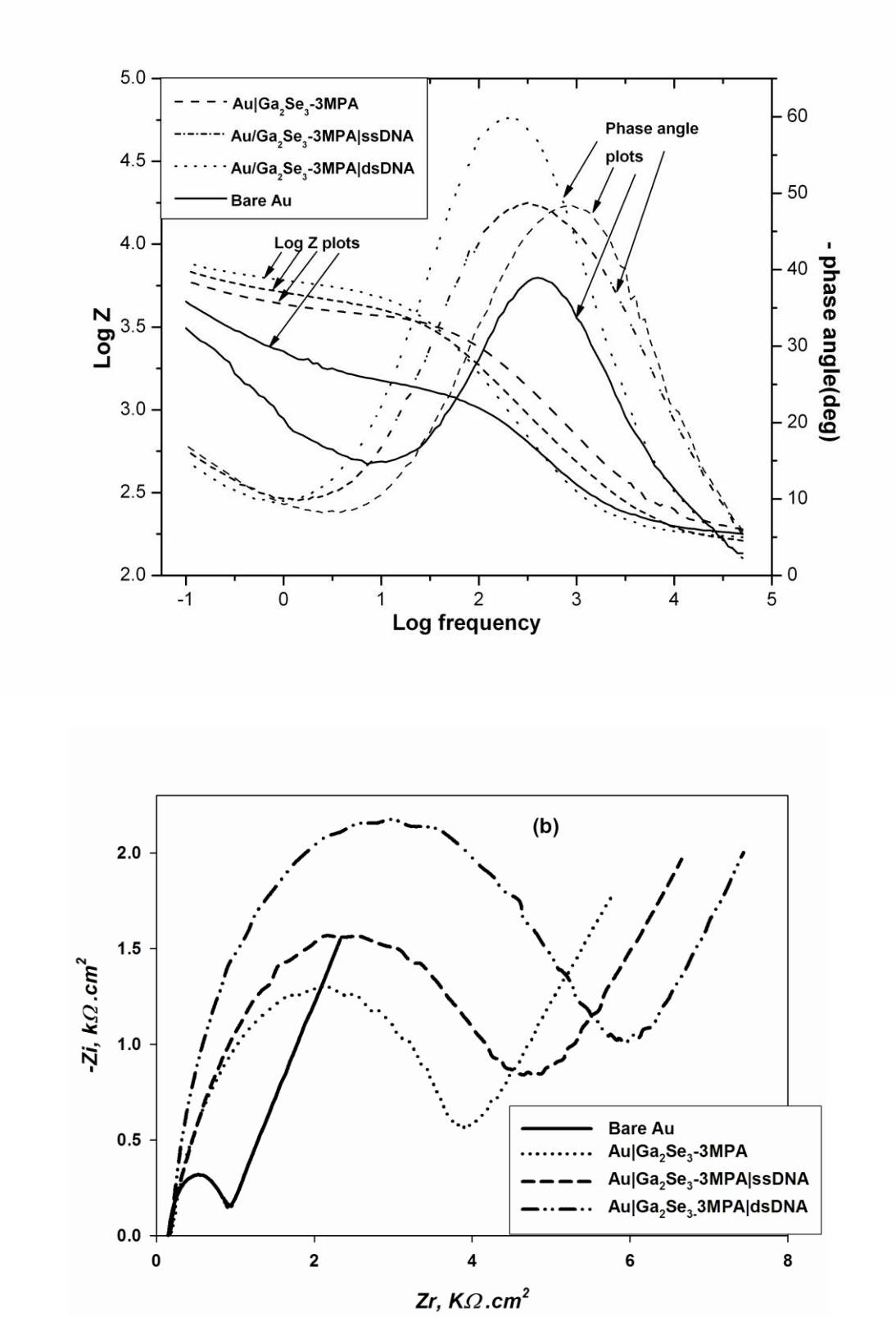

Figure 7. Bode (a) Nyquist (b) and plots of bare Au , Au|Ga_2Se_3-3MPA, Au| Ga_2Se_3-3MPA|ssDNA and Au| Ga_2Se_3-3MPA|dsDNA, all in 5.00 mM $Fe(CN)_6^{3-/4-}$.

The Bode plots show remarkable differences in the electrochemistry of the Au|Ga_2Se_3-3MPA|ssDNA-$Fe(CN)_6^{3-/4-}$ and Au|Ga_2Se_3-3MPA|dsDNA-$Fe(CN)_6^{3-/4-}$ interfaces. The absolute phase

angle increases from 49° (Au|Ga_2Se_3-3MPA|ssDNA) to 60° (Au|Ga_2Se_3-3MPA|dsDNA), accompanied by respective shift in the frequency of maximum phase angle ($\omega_{\varphi max}$) from 316 Hz to 200 Hz. This indicates decrease in conductivity at the Au|Ga_2Se_3-3MPA|dsDNA-$Fe(CN)_6^{3-/4-}$ interface. It can be explained by the accumulation of negative charge from the DNA backbone after hybridization which caused a higher barrier for the negatively charged $Fe(CN)_6^{3-/4-}$ anions and impeded the redox conversion at the electrode. From the Nyquist diagram, the diameters of the observed semicircles gave a first estimate of the charge transfer resistances, R_{ct}, at the two interfaces. The R_{ct} values were obtained by fitting the EIS data to the Randle's equivalent circuit shown in Figure 3. Compared to Au|Ga_2Se_3-3MPA electrode, Au|Ga_2Se_3-3MPA|ssDNA shows higher R_{ct} value (3548 ± 2.09 Ω), which is indicative of electrostatic repulsion between the polyanionic backbone of ssDNA and the anionic $Fe(CN)_6^{3-/4-}$. Hybridization with 20 nM complementary DNA induced a further increase in R_{ct} to 4436 ± 2.74 Ω, implying an increase in negative charge at the surface of the electrode. All the EIS spectra in Figure 6 are characterised by one semicircle as expected for the occurrence of a single redox process. For the Au|Ga_2Se_3-3MPA|dsDNA biosensor system, the R_{ct} value of the $Fe(CN)_6^{3-/4-}$ reports the dsDNA|$Fe(CN)_6^{3-/4-}$ interfacial kinetics. R_{ct} was, therefore, taken as the analytical parameter for the impedimetric detection of the target DNA.

3.4. Analytical performance of the impedimetric genosensor

Figure 8 shows the Nyquist plots obtained with the Au|Ga_2Se_3-3MPA|ssDNA electrode after dipping it into a stirred solution (0.10 M phosphate buffer, pH 7.40) containing different concentrations of the target DNA while holding the potential at 500 mV for 6 min. The R_{ct} values increased with increasing concentration of the target DNA. The change in R_{ct} (i.e. $\Delta R_{ct} = R_{ct(dsDNA)} - R_{ct(ssDNA)}$) gave a linear relationship with the logarithm of the concentration of the target DNA within a concentration range of 20 - 140 nM (Fig 9).

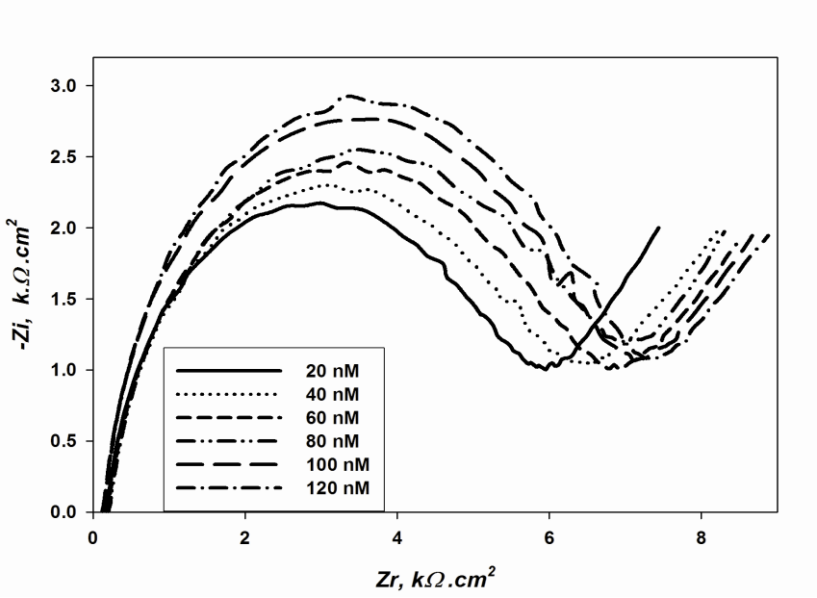

Figure 8. Nyquist plots of Au|Ga_2Se_3-3MPA|ssDNA responses to target DNA in 5.00 mM $Fe(CN)_6^{3-/4}$.

The sensitivity of the genosensor was found to be 11.61 Ω/nM (r^2 = 0.99) and a detection limit of 0.66 nM (3s, n = 8). The stability of the Au|Ga_2Se_3-3MPA|ssDNA genosensor was studied by measuring its impedimetric response to 100 nM target DNA concentration at different storage intervals for one month, storing it in phosphate buffer, pH 7.40 at 4 °C between measurements. It was found to lose 28 % of its response within this time. 10 separate Au|Ga_2Se_3-3MPA|ssDNA genosensors were prepared and used for storage stability and reproducibility studies. The impedimetric responses of each of the 10 genosensors to 100 nM target DNA were measured at different storage times, ranging from one day to one month. The sensor showed only 17% loss in response after a storage time of one month. The 10 genosensors exhibited excellent reproducibility giving an average ΔR_{ct} value of 2620 Ω with a standard deviation of 2.36 Ω. This is in agreement with the ΔR_{ct} value for 100 nM target DNA shown in Fig. 9.

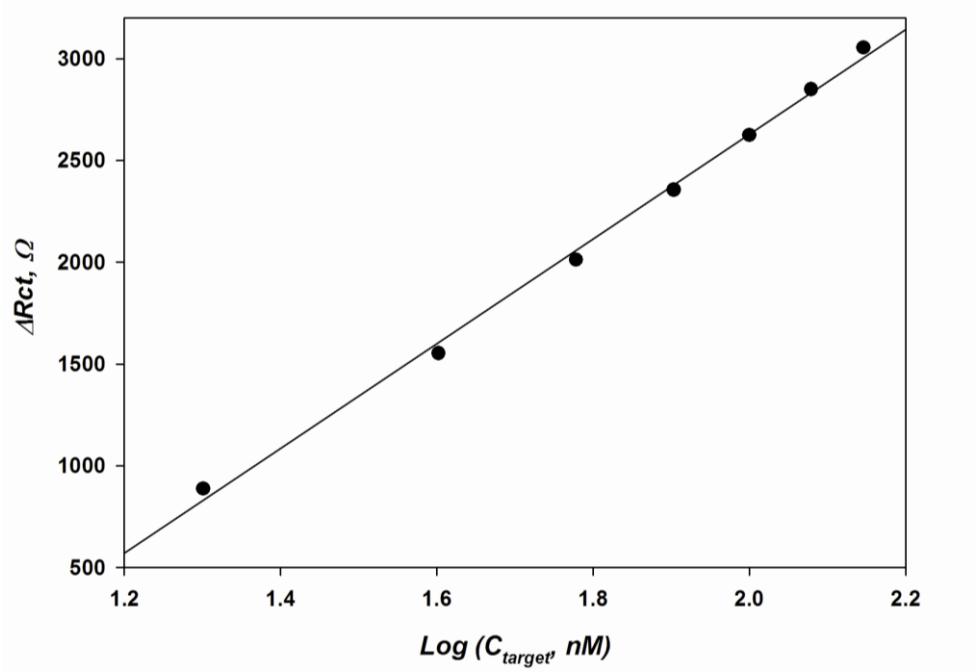

Figure 9. Calibration plot for the genosensor

3.5. Discrimination among complementary, non-complementary and 3-base mismatch target sequences

Hybridization experiments were performed with complementary, non-complementary and 3-base mismatched target sequences as samples and their corresponding $R_{ct(sample)}$ values were calculated from the impedimetric data. The resultant impedimetric signals were analysed as the ratio of change in R_{ct} {i.e. $\Delta R_{ct(ratio)} = (R_{ct(sample)} - R_{ct(blank)})/(R_{ct(probe)} - R_{ct(blank)})$}, where $R_{ct(blank)}$ is the value for bare Au and $R_{ct(probe)}$ is the value for genosensor. A $\Delta R_{ct(ratio)} > 1$ indicates the occurrence of hybridization

reactions and $\Delta R_{ct(ratio)} \leq 1$ is an indicator of non-hybridization reactions or nonspecific adsorption [14]. The complimentary DNA gave $\Delta R_{ct(ratio)} > 1$ which is attributed to specific hybridization reaction between the probe DNA and the complementary DNA (5′-GAACATGAAGGACCGGTGGG-3′). The 3-base mismatch and non-complimentary DNAs gave $\Delta R_{ct(ratio)} \approx 0.85$, showing that they did not hybridize with the genosensor.

4. CONCLUSION

This study demonstrated the genosensor application of a novel water soluble and biocompatible Ga_2Se_3-3MPA nanocrystals. A label free impedimetric genosensor fabricated on the nanocrystal modified gold electrode exhibited high sensitivity towards the target DNA (sensitivity = 11.61 Ω/nM) with a detection limit of 0.66 nM (3s, n = 8). It was able to discriminate between complementary, non-complementary and 3-base mismatch target sequences and maintained 87 % of its response towards the target DNA after one month.

ACKNOWLEDGEMENTS
The support of this study by the National Research Foundation (NRF), South Africa is highly acknowledged.

References

1. T. P. Gujar, V. R. Shinde, J.-W. Park, H. K. Lee, K.-D. Jung, O.-S. Joo, *Electrochim. Acta,* 54,(2008) 829.
2. C. E. M. Campos, J. C. de Lima, T. A. Grandi, K. D. Machado, P. S. Pizani, *Solid State Commun.,* 126,(2003) 611.
3. K. Ueno, S. Tokuchi, K. Saiki, A. Koma, *J. Cryst. Growth,* 237-239,(2002) 1610.
4. A. C. Wright, J. O. Williams, A. Krost, W. Richter, D. R. T. Zahn, *J. Cryst. Growth,* 121,(1992) 111.
5. J.-H. Park, M. Afzaal, M. Helliwell, M. A. Malik, P. O'Brien, J. Raftery, *Chem.Mat.,* 15,(2003) 4205.
6. A. Märkl, M. von der Emde, C. Nowak, W. Richter, D. R. T. Zahn, *Surf. Sci.,* 331-333,(1995) 631.
7. M. A. Afifi, A. E. Bekheet, H. T. El-Shair, I. T. Zedan, *Physica B: Condens. Matter,* 325,(2003) 308.
8. M. Rusu, S. Wiesner, S. Lindner, E. Strub, J. R¨ohrich, RW¨urz, WFritsch, W. Bohne, T. Schedel-Niedrig, M. C. Lux-Steiner, C. Giesen, M. Heuken, *J. Phys.: Condens. Matter,* 15,(2003) 8185.
9. P. J. Durrant, B. Durrant, *Introduction to Advanced Inorganic Chemistry*. Wiley, New York, (1962).
10. J. Li, G. Zou, X. Hu, X. Zhang, *J. Electroanal. Chem.,* 625,(2009) 88.
11. F. Zhang, C. Li, X. Li, X. Wang, Q. Wan, Y. Xian, L. Jin, K. Yamamoto, *Talanta,* 68,(2006) 1353.
12. M. Liu, G. Shi, L. Zhang, Y. Cheng, L. Jin, *Electrochem. Commun.,* 8,(2006) 305.
13. Z. Wang, Q. Xu, H.-Q. Wang, Q. Yang, J.-H. Yu, Y.-D. Zhao, *Sens. Actuators B: Chemical,* 138,(2009) 278.
14. A. Bonanni, M. J. Esplandiu, M. del Valle, *Biosens. Bioelectron.,* 24,(2009) 2885.
15. J.-B. Raoof, M. S. Hejazi, R. Ojani, E. H. Asl, *Int. J. Electrochem. Sci.,* 4,(2009) 1436.

16. D. L. Pelletier, *Food policy*, 31,(2006) 570.
17. J. E. Losey, L. S. Rayor, M. E. Carter, *Nature*, 399,(1999) 214.
18. D. Saxena, S. Flores, G. Stotzky, *Nature*, 402,(1999) 480.
19. F. Widmer, R. J. Seidler, K. K. Donegan, G. L. Reed, *Mol. Ecol.*, 6,(1997) 1.
20. F. Gebhard, K. Smalla, *FEMS Microbiol Ecology*, 28,(1999) 261.
21. I. Hay, M.-J. Morency, A. Se´guin, *Can. J.Forest Res.*, 32,(2002) 977.
22. D. Quist, I. H. Chapela, *Nature*, 414,(2001) 541.
23. M. Vaı¨tilingom, H. Pijnenburg, F. Gendre, P. Brignon, *J. Agric. Food Chem.*, 47,(1999) 5261.
24. L.-C. Chiueh, Y.-L. Chen, D. Y.-C. Shih, *J. Food. Drug Anal.*, 10,(2002) 25.
25. H. R. Permingeat, M. I. Reggiardo, R. H. Vallejos, *J.Agric. Food Chem.*, 50,(2002) 4431.
26. P. S. Duggan, P. A. Chambers, J. Heritage, J. M. Forbes, *FEMS Microbiol. Lett.*, 191,(2000) 71.
27. J. C. Jennings, L. D. Albee, D. C. Kolwyck, J. B. Surber, M. L. Taylor, G. F. Hartnell, R. P. Lirette, K. C. Glenn, *Poult. Sci.*, 82,(2003) 371.
28. F. E. Ahmed, *Trends Biotechnol.*, 20,(2002) 215.
29. M. Minunni, S. Tombelli, E. Mariotti, M. Mascini, *Fresenius' J. Anal. Chem.*, 369 (2001) 589.
30. I. Mannelli, M. Minunni, S. Tombelli, M. Mascini, *Biosens. Bioelectron.*, 18,(2003) 129.
31. E. Giakoumaki, M. Minunni, S. Tombelli, I. E. Tothill, M. Mascini, P. Bogani, M. Buiatti, *Biosens. Bioelectron.*, 19,(2003) 337.
32. G. Feriotto, M. Borgatti, C. Mischiati, N. Bianchi, R. Gambari, *J.Agric. Food Chem.*, 50,(2002) 955.
33. D. Gerion, W. J. Parak, S. C. Williams, D. Zanchet, C. M. Micheel, A. P. Alivisatos, *J. Am. Chem. Soc.*, 124,(2002) 7070.
34. O. A. Arotiba, P. G. Baker, B. B. Mamba, E. I. Iwuoha, *Int. J. Electrochem. Sci.*, 2011,(2011) 673
35. T. G. Drummond, M. G. Hill, J. K. Barton, *Nat Biotech*, 21,(2003) 1192.
36. C. Fan, K. W. Plaxco, A. J. Heeger, *Trends Biotechnol.*, 23,(2005) 186.
37. J. Wang, *Anal. Chim. Acta*, 469,(2002) 63.
38. E. Palecek, *Talanta*, 56,(2002) 809.
39. D. Ozkan, A. Erdem, P. Kara, K. Kerman, J. Justin Gooding, P. E. Nielsen, M. Ozsoz, *Electrochem. Commun.*, 4,(2002) 796.
40. A. Erdem, K. Kerman, B. Meric, U. S. Akarca, M. Ozsoz, *Anal. Chim. Acta*, 422,(2000) 139.
41. K. Maruyama, J. Motonaka, Y. Mishima, Y. Matsuzaki, I. Nakabayashi, Y. Nakabayashi, *Sens. Actuators B: Chem.*, 76,(2001) 215.
42. T. R. R. Naik, H. S. B. Naik, *Int. J. Electrochem. Sci.*, 3 (2008) 409
43. G.-U. Flechsig, T. Reske, *Anal. Chem.*, 79,(2007) 2125.
44. O. Pänke, A. Kirbs, F. Lisdat, *Biosens. Bioelectron.*, 22,(2007) 2656.
45. G. Ziyatdinova, J. Galandova, J. Labuda, *Int. J.Electrochem.Sci.*, 3,(2008) 223.
46. M. Y. Vagin, A. A. Karyakin, T. Hianik, *Bioelectrochemistry*, 56,(2002) 91.
47. A. S. Sarac, M. Ates, B. Kilic, *Int. J. Electrochem. Sci.*, 3 (2008) 777
48. T.-Y. Lee, Y.-B. Shim, *Anal. Chem.*, 73,(2001) 5629.
49. H. Li, W. Y. Shih, W.-H. Shih, *Nanotechnology*, 18 (2007) 205604.
50. E. Sabatani, J. Cohen-Boulakia, M. Bruening, I. Rubinstein, *Langmuir*, 9,(1993) 2974.
51. C. S. Christian Henke, Andreas Janshoff, Gerhard Steffan, Heinrich Luftmann, Manfred Sieber, and Hans-Joachim Galla, *Anal. Chem.*, 68 (1996) 3158.
52. A. J. Bard, L. R. Faulkner, *Electrochemical methods: Fundamentals and applications*. Wiley, New York, ed. 2nd edition, (2000).
53. J. D. K. Gosser, *Cyclic Voltammetry :simulations and Analysis of Reaction Mechanisms*. VCH Publishers Inc., Newyork, (1993).
54. E. Laviron, *J.Electroanal. Chem.*, 100, 263.
55. R. Greef, R. Peat, L. M. Peter, D. Pletcher, J. Robinson, Eds., *Instruental methods in electrochemistry*, (Elis Horwood, New York, 1990).

56. K. I. Ozoemena. (Transworld Research Network, Kerala, 2007).
57. R. S. Nicholson, *Anal. Chem.*, 37,(1965) 1351.
58. N. P. Osipovich, A. Shavel, S. K. Poznyak, N. Gaponik, A. Eychmülle *J. Phys.Chem. B,* 110,(2006) 19233.
59. N. Gaponik, S. K. Poznyak, N. P. Osipovich, A. Shavel, A. Eychmüller, *Microchim. Acta,* 160,(2008) 327.